Transparent and Catalytic Carbon Nanotube Films

Jessika E. Trancik,[*,†,‡] **Scott Calabrese Barton,**[§,△] **and James Hone**[⊥]

Santa Fe Institute, Santa Fe, New Mexico 87501, Earth Institute, Department of Chemical Engineering, and Department of Mechanical Engineering, Columbia University, New York, New York 10025

ABSTRACT

We report on the synthesis of thin, transparent, and highly catalytic carbon nanotube films. Nanotubes catalyze the reduction of triiodide, a reaction that is important for the dye-sensitized solar cell, with a charge-transfer resistance as measured by electrochemical impedance spectroscopy that decreases with increasing film thickness. Moreover, the catalytic activity can be significantly enhanced by exposing the nanotubes to ozone in order to introduce defects. Ozone-treated, defective nanotube films could serve as catalytic, transparent, and conducting electrodes for the dye-sensitized solar cell. Other possible applications include batteries, fuel cells, and electroanalytical devices.

Carbon nanotubes combine advantages such as electrical conductivity, chemical stability, high surface area, and optoelectronic properties that make them excellent candidates for a variety of energy conversion and storage technologies.[1–7] In addition, carbon nanotubes have been shown to be electrochemically active in several systems.[1,8–15] For example, they are catalytic in the dye-sensitized solar cell (DSSC)[13,15] as well as in several electroanalytical applications[9,11] and serve as sites for catalysis and intercalation in hydrogen fuel cells and lithium ion batteries.[1,10,12,14] However, the electrochemical activity of carbon nanotube films is not well understood experimentally or theoretically. To further quantify the limits of electrochemical activity of these materials, it is important to control for nanotube loading, characterize carefully isolated nanotube electrodes (rather than examining whole devices where many factors other than the nanotubes themselves can contribute to device performance), and explore ways to optimize performance through processing.

In this study, we quantify the catalytic activity of single-walled carbon nanotube films in a model system, the DSSC. The DSSC consists of dye molecules chemically adsorbed on the surface of a TiO_2 nanoparticle network anode and a contacting redox active electrolyte, most commonly a solution containing iodide and triiodide molecules.[16,17] The cell anode serves as the current collector for the photogenerated electrons in the nanoparticle network, while the cathode injects charge into the electrolyte and catalyzes the reduction of triiodide:

$$I_3^- + 2e^- \leftrightarrow 3I^- \qquad (1)$$

The cathode is commonly made from a thin (1–5 nm) layer of platinum catalyst deposited on a transparent conducting oxide (TCO) such as fluorine tin oxide (FTO) on glass or indium tin oxide (ITO) on a glass or polymer substrate. A transparent cathode allows for straightforward use of low-cost, flexible substrates because the TiO_2 films can be sintered at high temperature on an opaque metallic film. A transparent cathode can also allow for construction of a tandem cell containing two or more separate compartments with dye molecules that absorb different parts of the solar spectrum, to achieve high efficiency cells and lower the cost of generated electricity.[18]

Previous work has shown that carbon nanotubes also catalyze the reduction of triiodide and thus may be able to replace platinum in the DSSC.[13] In this context, carbon nanotube films have several advantages. Platinum was found to degrade over time while in contact with an iodide/triiodide liquid electrolyte, reducing the efficiency of a DSSC, whereas carbon nanotubes did not degrade.[15] In addition, multiple papers demonstrate the high conductivity and transparency of carbon nanotubes films, which have reached performance approaching that of TCOs on rigid substrates and comparable to TCOs on flexible substrates.[2,4,19–24] This combination of properties means that carbon nanotubes may be able to replace the TCO layer used in the DSSC as well as the platinum catalyst. (The transparency and conductivity also gives carbon nanotube films an advantage over other alterna-

* Corresponding author. E-mail: trancik@santafe.edu. Telephone: +1 505 984 8800.
† Santa Fe Institute.
‡ Earth Institute, Columbia University.
§ Department of Chemical Engineering, Columbia University.
△ Department of Chemical Engineering and Materials Science, Michigan State University.
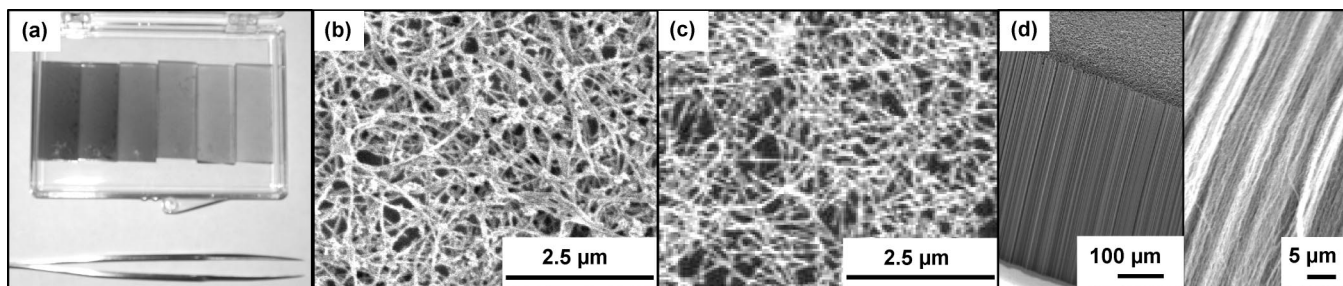⊥ Department of Mechanical Engineering, Columbia University.

Figure 1. Images of carbon nanotube films showing the effect of synthesis procedure on film morphology. (a) Photo of airbrushed films of varying thicknesses on a conducting glass substrate, made from nanotubes produced by arc discharge. Nanotubes were suspended in an ethanol solution and airbrushed on a conducting glass substrate. (b) Scanning electron microscope (SEM) image of films of arc discharge produced nanotubes. These films consist of short single-walled nanotube bundles, where the short tube length is a result of long sonication times.[39] (c) SEM image of a CVD grown mat film, where nanotubes are grown in the plane of the substrate. CVD mat films consist of long, single tubes. (d) SEM image of a CVD forest film, where nanotubes are grown perpendicular to the substrate. CVD forest films consist of multiwalled nanotubes (with a few walls) that can be transferred to a desired substrate by direct contact (typically by rubbing a wooden tip along the growth substrate and then the desired substrate) or can be put in solution and airbrushed on a substrate. Airbrushing of arc discharge tubes (a,b) yielded the most reproducable results and easiest deposition at a range of thicknesses and on a variety of substrates, and was therefore used for most of the electrochemical characterization unless otherwise specified.

tive catalysts, such as carbon black films, which have also been shown to be catalytic in the DSSC but are opaque and less conductive.[25]) Carbon nanotube films are much more flexible and less prone to cracking than TCOs, making them ideal candidates for inexpensive roll-to-roll processing and varied installation configurations.[19] Because the previous work in this area did not control for nanotube loading and focused on the efficiency of entire cells, where performance is sensitive to small changes in multiple cell components, the catalytic performance of nanotube films has not been measured directly and is therefore still unknown.

The purpose of this study is to quantify the catalytic activity of carbon nanotube films and to explore methods for increasing their electrochemical activity through film processing. We report measurements using electrochemical impedance spectroscopy (EIS) of the charge-transfer resistance R_{CT} associated with the reduction of triiodide as a function of film transparency and loading, and demonstrate that exposing the films to UV-generated ozone dramatically increases their catalytic activity, presumably by introducing defects. Ozone-treated tubes show high enough performance to replace platinum in the DSSC. We also develop a road map for simultaneously optimizing the transparency, conductivity, and catalytic activity of carbon nanotube films. These films could be used to replace both platinum and a TCO in the DSSC.

We deposited films from single-walled carbon nanotubes (Carbon Solutions Inc.) produced using arc discharge (Figure 1). The tubes contain metal impurities consisting of nickel and yttrium in a ratio of approximately 3:1 atom %, totaling approximately 7% by weight as determined by thermal gravimetric analysis. In addition to single-walled nanotubes, the samples include carbonaceous impurities in the form of amorphous carbon and graphitic nanoparticles of less than 10 wt % (defined in terms of relative purity and characterized using near-infrared spectroscopy[26]). Films were suspended in a variety of solvents, sonicated for 16 h, and airbrushed onto a substrate placed on a hot plate at 100–150 °C. An ethanol solvent combined with airbrushing yielded the most

reproducible results and easiest deposition on a variety of substrates and was therefore used for electrochemical characterization. Although the nanotube films were conducting on their own, a conducting substrate (glass coated with F:SNO$_2$ (FTO), sheet resistance of 15 Ω/□) was used to obtain reliable electrochemical data from nanotube films with a wide range of thicknesses by ensuring that all films had a constant, low ohmic resistance. The FTO films do not on their own catalyze the reduction of triiodide and therefore do not interfere with electrochemical data (see Supporting Information).

We also used chemical vapor deposition (CVD) (see Supporting Information) to grow both mats and forests of tubes (Figure 1). The mats consist of long, single-walled nanotubes that are oriented along the plane of the substrate and were used to demonstrate our ability to vary tube length and thereby optimize conductivity of the films. The forest samples yield few-walled tubes that are oriented perpendicular to the substrate[27] and are used to make ultrapure films, due to the extremely low metal (iron) to carbon ratio (metal content <0.01 wt %). By transferring a film of the forest tubes to a conducting glass substrate (using either direct contact or airbrushing tubes in an ethanol solution) and characterizing these samples using EIS, it was possible to investigate the impact of metal impurities on the catalytic activity of the films. (Note that the films made from airbrushed, arc discharge tubes were the most evenly distributed and therefore the bulk of the electrochemical data is recorded from these samples, unless otherwise specified.) For comparison purposes, we also deposited thin layers of platinum (1–5 nm) on FTO using e-beam evaporation. The light transmittance of all films was measured using UV–visible spectroscopy (Cary 50 Bio UV–visible spectrophotometer).

Using EIS, we then characterized the catalytic activity of carbon nanotube films for reduction of triiodide. A three-electrode cell, providing strict control of electrode potential,[28] was used to measure the charge-transfer resistance R_{CT} at the carbon nanotube/electrolyte interface: R_{CT} indicates the
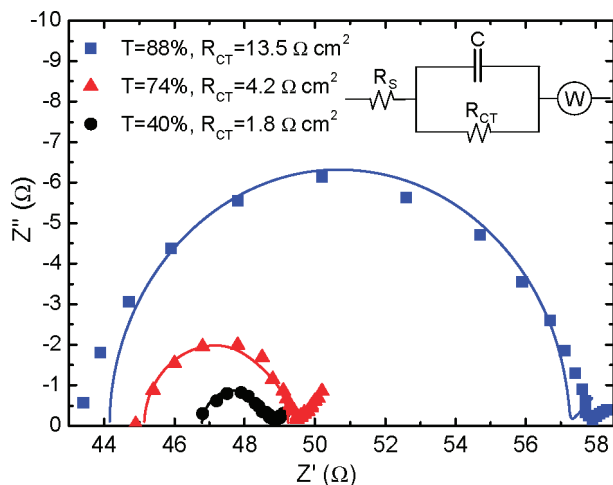
Figure 2. Charge-transfer resistance (R_{CT}) decreases with increasing film thickness, indicating that thicker films are more catalytic. Nyquist plots are shown here for airsprayed carbon nanotube films with varied loading. Measurements were made at 300 mV in order to avoid the mass transport limited regime. The frequency range was 0.1−100000 Hz, with frequency decreasing from left to right along the x-axis, however high frequency points below the x-axis are not shown here. The decreasing radius of the semicircle shown indicates a decrease in R_{CT}. The inset shows the equivalent circuit used to model this system, including a component R_s = series resistance, R_{CT} = the charge-transfer resistance, C = double layer capacitance, and W = Warburg impedance. Transmittance values are for the carbon nanotube film alone. (The contribution from the FTO layer has been subtracted.) Current–voltage curves are shown in the Supporting Information.

electron transfer resistance and thus varies inversely with the triiodide reduction activity of the carbon nanotubes. The cell consisted of a working electrode (carbon nanotube film + FTO + glass), a reference electrode (Ag/AgCl), and a counter-electrode (platinum wire). The electrolyte was 0.05 M I_2 + 0.5 M LiI in aqueous solution.[29] Nonaqueous solutions are often employed in the DSSC due to lower efficiencies exhibited by aqueous cells. There have been recent efforts, however, to optimize the efficiency of aqueous cells because of their potential as low-cost, environmentally friendly substitutes for the volatile and flammable nonaqueous electrolytes.[30] A nonaqueous acetonitrile (CH_3CN) based electrolyte solution was also used here but offered less reproducibility and stability. Therefore trends in the catalytic activity of the carbon nanotube films are presented from testing in an aqueous solution. Measurements were made with a Schlumberger SI 1255 HF frequency response analyzer and an EG+G Princeton Applied Research potentiostat/galvanostat model 273A. Cell measurements were taken at a working electrode potential of 300 mV, away from the mass-transport limited region, and over a frequency range of 0.1−100000 Hz.

We observed that R_{CT} at the electrolyte and carbon nanotube interface decreases with increasing carbon nanotube loading and decreasing light transmittance. This can be seen in the Nyquist plots shown in Figure 2 for films with transmittance ranging from 40 to 90% and R_{CT} ranging from 1.8 to 13.5 Ω cm². This difference is due to the increase in surface area of the carbon nanotube films with higher

nanotube loading. The plots were fitted with the equivalent circuit shown in Figure 2, consisting of the R_{CT} and in parallel a double layer capacitance C, both of which are in series with the Warburg impedance W and series resistance R_s. C increases systematically with nanotube loading as expected due to an increase in active surface area (see Supporting Information). R_s includes the ohmic resistance of the electrolyte, the conducting substrate, and nanotube film layers and does not vary significantly with nanotube loading. The Warburg impedance arises from mass transport limitations due to diffusion in the electrolyte and does not vary significantly with nanotube loading. (Current–voltage curves for these samples are shown in the Supporting Information.)

As-deposited nanotubes display significant catalytic activity. For instance, the thickest film ($T = 40\%$ and nanotube loading ∼0.15 mg/cm²) has a charge-transfer resistance of 1.8 Ω cm², a value that is comparable to that achieved by opaque carbon black films of ∼10–20 μm thickness (loading ∼1–2 mg/cm²).[25] (Note that this comparison takes into account differences in absolute values of R_{CT} due to the nonaqueous electrolyte used in the carbon black study.) In fact, the R_{CT} of the thicker carbon nanotube films approaches that of a thin layer of platinum (∼0.5 Ω for a 1 nm e-beam evaporated film), albeit with lower transparency.

Previous current–voltage simulation results have suggested that surface defect sites, in particular edge-plane-like defect sites, are responsible for much of the catalytic activity, electron transfer, and chemical reactivity of graphitic carbon including carbon nanotubes.[9] Furthermore, ozone treatment of carbon nanotubes has been shown in previous work, using Raman spectroscopy and X-ray photoelectron spectroscopy, to lead to increased defect density due to sidewall oxidation, resulting in irreversible increases in the electrical resistance of tubes.[31] For example, Raman spectra showed that the ratio of the D-band to the G-band increased linearly with ozone exposure time. Therefore, we exposed our films to UV-generated ozone (UVOCS UV ozone cleaner) in order to introduce defects and study the resulting changes in catalytic activity.

We found that, for a given film thickness, R_{CT} decreased with ozone exposure (applied in 10 min intervals) up to 20 min and then increased after further ozone treatment (Figure 3). The magnitude of the decrease in R_{CT} is greater for thin samples. For example, for a ∼0.015 mg/cm² sample, R_{CT} decreased from 88.4 to 9.4 Ω cm² after 20 min of ozone exposure. The light transmittance of all films increased only slightly after 10 min of ozone exposure and more dramatically for longer exposures. We also observed that the sheet resistance of films on insulating substrates changed only slightly with short ozone exposure times and then increased significantly for longer exposures (see Supporting Information). These results suggest that short ozone exposure (≤20 min) introduces defects that increase the catalytic activity of the nanotubes without significantly changing either the light transmission or sheet resistance. Longer exposure begins to remove tubes, increasing the transmittance, sheet resistance, and R_{CT}.
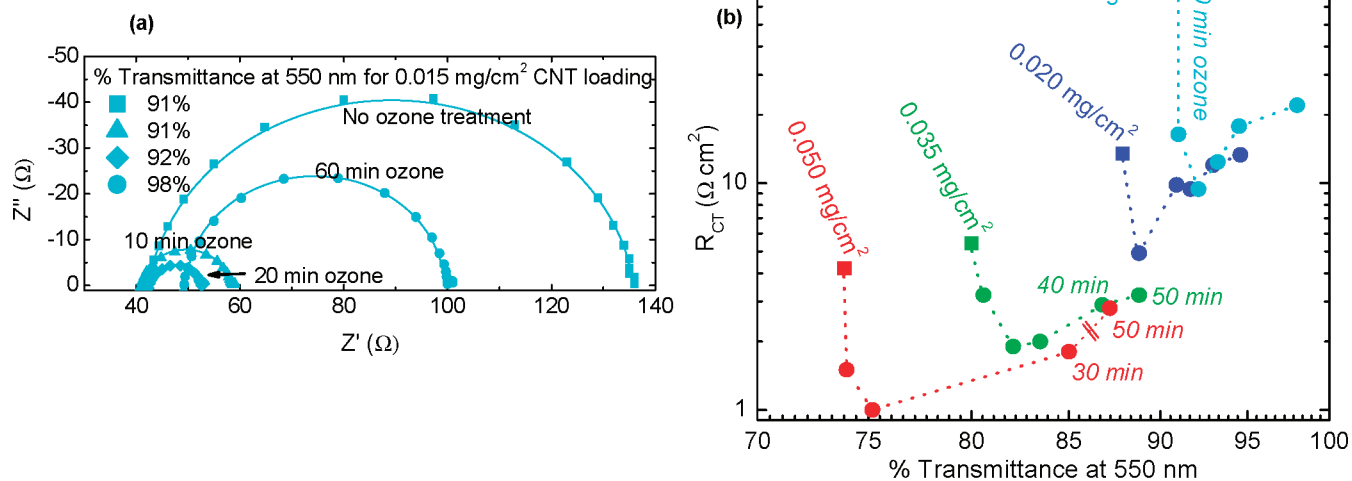
Figure 3. Carbon nanotube films become more catalytic with ozone treatment. Results are shown for airbrushed films of nanotubes produced using arc discharge (Figure 1a,b). (a) Nyquist plots are shown for an ozone-treated carbon nanotube film with ~0.015 mg/cm² loading. The decreasing radius of the semicircle indicates a decrease in R_{CT}. The equivalent circuit is shown in Figure 2. Current–voltage curves are shown in the Supporting Information. (b) R_{CT} and T for films with varied nanotube loading and ozone treatment lengths. R_{CT} decreases initially and then begins to increase with longer ozone treatment durations. T increases with treatment duration. (Transmittance values are for the carbon nanotube film alone.) The colors indicate samples with different nanotube loading. Squares signify untreated samples; circles indicate samples that have been treated with UV-generated ozone. The minutes of ozone treatment duration are shown for samples that are within an approximate target region of suitability for the DSSC. The data point for the ~0.050 mg/cm² sample exposed to ozone for 40 min was left out due to poor measurement quality. The data point for the untreated ~0.035 mg/cm² sample has a large error in R_{CT} (~10%) due to poor measurement quality. The far lower right region of low charge-transfer resistance and high transmittance is optimal.

As an additional check, we tested the effect of ozone treatment in an acetonitrile (CH_3CN) based, nonaqueous solution in order to determine whether the treatment was simply making the tubes more hydrophilic. An initial decrease and then increase in the charge-transfer resistance with increasing ozone treatment duration was seen in these samples as well (see Supporting Information).

The observed results are also inconsistent with other proposed mechanisms for catalysis, such as electrochemical activity, which is dominated by the metal impurities remaining in the nanotube samples.[32–34] Metal impurities, which are sheathed by several graphene sheets, can remain in nanotube samples after purification procedures.[35] These impurities have been shown to be a significant factor in the electrochemical activity of carbon nanotubes in certain systems such as for the reduction of hydrogen peroxide.[33] To test the possible effect of metal impurities (in the case of films presented in Figure 3, the impurities are nickel particles) on the electrochemical activity, we studied ultrapure carbon nanotube films from forests grown by CVD (Figure 1d). The ultrapure films exhibit similar behavior to the films made from arc discharge produced nanotubes. As shown in Figure 4, we observe a significant decrease in R_{CT} after ozone exposure. Therefore, these results strongly support a model of catalysis at defect sites, a phenomenon that will be interesting to study further in a wide variety of systems beyond the DSSC.

One attractive feature of the ozone treatment technique is that it allows one to study a carefully controlled film morphology that is similar before and after treatment, apart from the structural changes induced by the treatment. The technique can be used to study electrochemical activity of single tubes or dense films and is less intrusive than other methods for inducing disorder in carbon nanotubes, such as ball milling and prolonged sonication in acid solutions,[12,36,37] which require redeposition of the film, thus greatly modifying the original film morphology.

In addition to its effectiveness for basic characterization of the electrochemical effects of defects, ozone treatment also has practical benefits as a processing technique. It is easy to control the exact degree of treatment intensity by varying duration. Also, ozone treatment is likely to be more economically viable than the other processes mentioned; it does not require additional solution processing steps and does not waste tubes. We anticipate that ozone processing may be useful for increasing the efficiency of carbon nanotube electrodes for electrochemical photovoltaic cells, as well as for batteries, fuel cells, and electroanalytical devices, where defects are expected to be important for lithium intercalation, for catalyzing the reduction of oxygen, and for sensing chemical species.[1,9–12,14,36,38]

We also tested the effect of ozone treatment for a graphite sample in aqueous solution and found that R_{CT} decreased (see Supporting Information). This suggests that ozone treatment could be a useful and inexpensive procedure for increasing the electrochemical activity of graphitic carbon materials in a variety of configurations. Single-walled carbon nanotubes, however, may offer the most attractive combination of multiple properties: transmittance, conductance, and catalytic activity.

In the final part of this study, we asked whether a carbon nanotube film could be employed in a DSSC as a
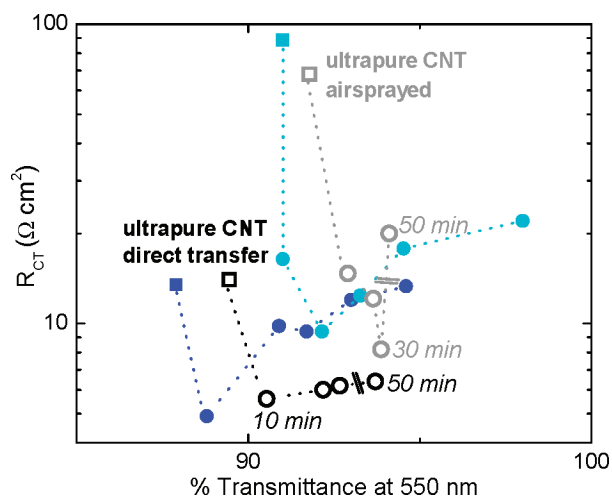
Figure 4. Films made from few-walled, carbon nanotube forests that are grown via chemical vapor deposition (Figure 1d) and are ultrapure (metal content <0.01 wt %) also become more catalytic with ozone treatment. Results are shown for an airbrushed film where tubes were suspended in ethanol (grey symbols) and a film that has been directly transferred from the growth substrate to the conducting glass substrate (black symbols). R_{CT} and T are presented for films with varied ozone treatment lengths. R_{CT} decreases initially and then increases with longer ozone treatment durations. T increases with treatment duration. (Transmittance values are for the carbon nanotube film alone. Note that due to the uneven nature of the airbrushed film made from forest tubes, indicated by grey symbols, the transmittance values are more uncertain than for other films.) These results are overlaid on those presented in Figure 3 for airbrushed films from arc discharge produced nanotubes, in order to show that both types of films show similar behavior. This confirms that the catalytic properties seen here are not dominated by metal impurities. Nyquist plots are shown in the Supporting Information.

transparent, conducting, and catalytic layer, replacing both the TCO and platinum. Recent experimental work has demonstrated carbon nanotube films with performance comparable to that of TCOs on flexible substrates and approaching that of TCOs on rigid substrates.[2,4,19–24] Further increases in conductivity and light transmittance should be possible for films with longer tubes; the light transmittance to sheet resistance ratio is expected to increase with tube length up to a limit where the resistance of the tubes themselves dominates that of the junctions between tubes, estimated at a length of 20–30 μm.[39] Up to this threshold, theory predicts and experiments on single-walled nanotube bundles ranging in length from ~0.4 to 4 μm have shown,

that the conductivity of a film will increase as a function of the length of tubes following a power law with an exponent of ~1.5.[39] Well-dispersed films with an average tube length of 25 μm should, based on this relationship, exhibit a sheet resistance (R_s) of ~20 Ω/□ at a light transmittance of ~90%. At these levels, the film would perform comparably to that of a TCO on glass and better than TCOs on flexible substrates[40] (Table 1). (The performance of TCOs on flexible substrates is limited by challenges in depositing uniform TCO films at low temperatures. Carbon nanotube films can, however, easily be deposited on a variety of substrates, either through direct deposition (airbrushing) or by using a transfer procedure following vacuum filtration or CVD growth.[24]) Lower sheet resistance levels may be achievable with high fractions of metallic to semiconducting tubes. The nature of the nanotube junctions is also expected to be an important determinant of conductivity.[23]

The experimental challenge is to develop carbon nanotube films that consist of long tubes and where the loading is high enough to achieve low sheet resistances. This could be achieved by growing thick CVD mat films (thicker than that shown in Figure 1c) or developing filtered and airbrushed films that can be evenly distributed across a substrate surface without requiring long sonication times. We have obtained preliminary results in this area.

A target catalytic, transparent, and conductive nanotube sample, which performs close to comparably to a TCO and platinum on glass and may outperform these films on flexible substrates, is shown in Table 1. This assumes an underlying, highly conductive layer of tubes that has been coated with a layer of ozone-treated tubes.

In summary, we have shown that carbon nanotube films are effective at catalyzing the reduction of triiodide and that the catalytic strength of thin films can be greatly enhanced by exposing the nanotubes to UV-generated ozone in order to introduce defects. Furthermore, we outline a road map for synthesizing carbon nanotube electrodes that are transparent, conductive, and catalytic, for application in the dye-sensitized solar cell. Other possible applications for ozone-treated catalytic carbon nanotube films include lithium ion batteries, hydrogen fuel cells, and electroanalytical instruments.

Table 1. Light Transmittance, Charge-Transfer Resistance, and Sheet Resistances for Various Films

sample	% light transmittance at 550 nm	charge-transfer resistance R_{CT} (Ω cm²)	sheet resistance R_{sq} (Ω/□)
FTO + glass	82.4	very high	15
FTO + 1 nm Pt + glass	80.4	≤0.5	15
FTO + 5 nm Pt + glass	67.1	<0.5	15
ITO + 1 nm Pt + polymer	78	<0.5	60–250
target CNT film on polymer or glass[a]	80	2–3	20

[a] This is a target film for replacing FTO or ITO + Pt in a DSSC. CNT = carbon nanotube. This film should be well within an achievable range but has not yet been demonstrated experimentally. The assumptions are the following: bottom layer tube length of 25 μm leading to a reduced sheet resistance following the relationship determined by Hecht et al.;[39] top layer is a CNT film with a loading of ~0.035–0.050 mg/cm² treated with ozone for 30–50 min. Note that it may be worth using a carbon nanotube film with somewhat higher initial R_{CT} value than platinum in order to avoid seasoning, which has been shown to decrease the efficiency of a DSSC up to 2–4% depending on the platinum deposition method used.[15]

Supporting Information Available: Additional description of carbon nanotube film synthesis methods and further characterization of catalysis, transparency, and conductivity. This material is available free of charge via the Internet at http://pubs.acs.org.

References

 (1) Che, G. L.; Lakshmi, B. B.; Fisher, E. R.; Martin, C. R. *Nature* **1998**, *393*, 346.
 (2) Hu, L.; Hecht, D. S.; Gruner, G. *Nano Lett.* **2004**, *4*, 2513.
 (3) Planeix, J. M.; Coustel, N.; Coq, B.; Brotons, V.; Kumbhar, P. S.; Dutartre, R.; Geneste, P.; Bernier, P.; Ajayan, P. M. *J. Am. Chem. Soc.* **1994**, *116*, 7935.
 (4) Wu, Z.; Chen, Z.; Du, X.; Logan, J. M.; Sippel, J.; Nikolou, M.; Kamaras, K.; Reynolds, J. R.; Tanner, D. B.; Hebard, A. F.; Rinzler, A. G. *Science* **2004**, *305*, 1273.
 (5) Guldi, D. M. *Phys. Chem. Chem. Phys.* **2007**, *9*, 1400.
 (6) Kamat, P. V. *Nano Today* **2006**, *1*, 20.
 (7) Kongkanand, A.; Dominguez, R. M.; Kamat, P. V. *Nano Lett.* **2007**, *7*, 676.
 (8) Nugent, J. M.; Santhanam, K. S. V.; Rubio, A.; Ajayan, P. M. *Nano Lett.* **2001**, *1*, 87.
 (9) Banks, C. E.; Davies, T. J.; Wildgoose, G. G.; Compton, R. G. *Chem. Commun.* **2005**, xxx829.
 (10) Britto, P. J.; Santhanam, K. S. V.; Rubio, A.; Alonso, J. A.; Ajayan, P. M. *Adv. Mater.* **1999**, *11*, 154.
 (11) Katz, E.; Willner, I. *ChemPhysChem* **2004**, *5*, 1084.
 (12) Meunier, V.; Kephart, J.; Roland, C.; Bernholc, J. *Phys. Rev. Lett.* **2002**, *88*, 075506.
 (13) Suzuki, K.; Yamaguchi, M.; Kumagai, M.; Yanagida, S. *Chem. Lett.* **2003**, *32*, 28.
 (14) Terrones, M. *Annu. Rev. Mater. Res.* **2003**, *33*, 419.
 (15) Koo, B.-K.; Lee, D.-Y.; Kim, H.-J.; Lee, W.-J.; Song, J.-S.; Kim, H.-J. *J. Electroceram.* **2006**, *V17*, 79.
 (16) O'Regan, B.; Grätzel, M. *Nature* **1991**, *353*, 737.
 (17) Wang, Q.; Ito, S.; Gratzel, M.; Fabregat-Santiago, F.; Mora-Sero, I.; Bisquert, J.; Bessho, T.; Imai, H. *J. Phys. Chem. B* **2006**, *110*, 25210.
 (18) Durr, M.; Bamedi, A.; Yasuda, A.; Nelles, G. *Appl. Phys. Lett.* **2004**, *84*, 3397.
 (19) Saran, N.; Parikh, K.; Suh, D.-S.; Munoz, E.; Kolla, H.; Manohar, S. K. *J. Am. Chem. Soc.* **2004**, *126*, 4462.
 (20) Zhang, M.; Fang, S.; Zakhidov, A. A.; Lee, S. B.; Aliev, A. E.; Williams, C. D.; Atkinson, K. R.; Baughman, R. H. *Science* **2005**, *309*, 1215.
 (21) Kaempgen, M.; Duesberg, G. S.; Roth, S. *Appl. Surf. Sci.* **2005**, *252*, 425.
 (22) Lee, K.; Wu, Z.; Chen, Z.; Ren, F.; Pearton, S. J.; Rinzler, A. G. *Nano Lett.* **2004**, *4*, 911.
 (23) Ma, W.; Song, L.; Yang, R.; Zhang, T.; Zhao, Y.; Sun, L.; Ren, Y.; Liu, D.; Liu, L.; Shen, J.; Zhang, Z.; Xiang, Y.; Zhou, W.; Xie, S. *Nano Lett.* **2007**, *7*, 2307.
 (24) Zhou, Y.; Hu, L.; Gruner, G. *Appl. Phys. Lett.* **2006**, *88*, 123109.
 (25) Murakami, T. N.; Ito, S.; Wang, Q.; Nazeeruddin, M. K.; Bessho, T.; Cesar, I.; Liska, P.; Humphry-Baker, R.; Comte, P.; Pechy, P.; Gratzel, M. *J. Electrochem. Soc.* **2006**, *153*, A2255.
 (26) Itkis, M. E.; Perea, D. E.; Niyogi, S.; Rickard, S. M.; Hamon, M. A.; Zhao, B.; Haddon, R. C. *Nano Lett.* **2003**, *3*, 309.
 (27) Hata, K.; Futaba, D. N.; Mizuno, K.; Namai, T.; Yumura, M.; Iijima, S. *Science* **2004**, *306*, 1362.
 (28) Hoshikawa, T.; Yamada, M.; Kikuchi, R.; Eguchi, K. *J. Electroanal. Chem.* **2005**, *577*, 339.
 (29) Hauch, A.; Georg, A. *Electrochim. Acta* **2001**, *46*, 3457.
 (30) Murakami, T. N.; Saito, H.; Uegusa, S.; Kawashima, N.; Miyasaka, T. *Chem. Lett.* **2003**, *32*, 1154.
 (31) Simmons, J. M.; Nichols, B. M.; Baker, S. E.; Marcus, M. S.; Castellini, O. M.; Lee, C.-S.; Hamers, R. J.; Eriksson, M. A. *J. Phys. Chem. B* **2006**, *110*, 7113.
 (32) Eugenii Katz, I. W. *ChemPhysChem.* **2004**, *5*, 1084.
 (33) Sljukic, B.; Banks, C. E.; Compton, R. G. *Nano Lett.* **2006**, *6*, 1556.
 (34) Kruusma, J.; Mould, N.; Jurkschat, K.; Crossley, A.; Banks, C. E. *Electrochem. Commun.* **2007**, *9*, 2330.
 (35) Pumera, M. *Langmuir* **2007**, *23*, 6453.
 (36) Gao, B.; Bower, C.; Lorentzen, J. D.; Fleming, L.; Kleinhammes, A.; Tang, X. P.; McNeil, L. E.; Wu, Y.; Zhou, O. *Chem. Phys. Lett.* **2000**, *327*, 69.
 (37) Liu, J.; Rinzler, A. G.; Dai, H.; Hafner, J. H.; Bradley, R. K.; Boul, P. J.; Lu, A.; Iverson, T.; Shelimov, K.; Huffman, C. B.; Rodriguez-Macias, F.; Shon, Y.-S.; Lee, T. R.; Colbert, D. T.; Smalley, R. E. *Science* **1998**, *280*, 1253.
 (38) Dai, G. P.; Liu, C.; Liu, M.; Wang, M. Z.; Cheng, H. M. *Nano Lett.* **2002**, *2*, 503.
 (39) Hecht, D.; Hu, L.; Gruner, G. *Appl. Phys. Lett.* **2006**, *89*, 133112.
 (40) Sheldahl Accentia Product Line Specifications (http://www.sheldahl.com).

NL071945I